Published in final edited form as:
Sci Transl Med. 2019 September 18; 11(510): . doi:10.1126/scitranslmed.aav5055.

Adipose tissue-derived WNT5A regulates vascular redox signaling in obesity via USP17/RAC1-mediated activation of NADPH oxidases

Ioannis Akoumianakis[#1], **Fabio Sanna**[#1], **Marios Margaritis**[1], **Ileana Badi**[1], **Nadia Akawi**[1], **Laura Herdman**[1], **Patricia Coutinho**[1], **Harry Fagan**[1], **Alexios S Antonopoulos**[1], **Evangelos K Oikonomou**[1], **Sheena Thomas**[1], **Amy P Chiu**[1], **Surawee Chuaiphichai**[1], **Christos P Kotanidis**[1], **Constantinos Christodoulides**[3], **Mario Petrou**[2], **George Krasopoulos**[2], **Rana Sayeed**[2], **Lei Lv**[1], **Ashley Hale**[1], **Meisam Naeimi Kararoudi**[1], **Eileen McNeill**[1], **Gillian Douglas**[1], **Sarah George**[4], **Dimitris Tousoulis**[5], **Keith M Channon**[1], **Charalambos Antoniades**[1,‡]

[1]Division of Cardiovascular Medicine, University of Oxford, Oxford, OX3 9DU, UK

[2]Department of Cardiothoracic Surgery, Oxford University Hospitals NHS Trust, Oxford, OX3 9DU, UK

[3]Oxford Centre for Diabetes, Endocrinology and Metabolism, University of Oxford, Oxford, OX3 7LE, UK

[4]Bristol Medical School, Research Floor Level 7, Bristol Royal Infirmary, Bristol, BS2 8HW, UK

[5]Cardiology Department, Athens University Medical School, Athens, 115 27, Greece

[#] These authors contributed equally to this work.

Abstract

[‡]Corresponding author. antoniad@well.ox.ac.uk.

Author contributions

I.A. conceived and performed experiments, contributed to participant recruitment, performed data analysis and drafted the manuscript; F.S. conceived and performed experiments, performed data analysis and contributed to the writing of the manuscript; M.M. performed experiments, contributed to participant recruitment, performed data analysis and reviewed the manuscript; I.B. performed experiments and reviewed the manuscript; N.A. performed data analysis and reviewed the manuscript; LH. Contributed to participant recruitment, data collection and analysis; P.C. performed experiments; H.F. performed experiments; A.S.A. contributed to participant recruitment, performed experiments and data analysis and reviewed the manuscript; E.K.O. contributed to participant recruitment and reviewed the manuscript; S.T. contributed to participant recruitment and data collection; A.P.C performed experiments and reviewed the manuscript; S.C. performed experiments; C.P.K. performed experiments; C.C. provided experimental resources and expertise and reviewed the manuscript; M.P. contributed to surgical specimen collection; G.K. contributed surgical specimen collection; R.S. contributed to surgical specimen collection; L.L. performed experiments; A.H. provided experimental resources and expertise; M.K. performed experiments; E.M. provided experimental resources and expertise; G.D. provided experimental resources and expertise; S.G. provided expertise and reviewed the manuscript; D.T. contributed to data analysis and reviewed the manuscript; K.M.C. contributed to the project design, provided experimental resources and expertise and reviewed the manuscript; C.A. conceived the project, secured funding, oversaw the implementation of individual experiments, performed data analysis and corrected the manuscript.

Competing interests:

C.A. and K.M.C are founders, shareholders and directors of Caristo Diagnostics, a CT Image analysis spinout company from the University of Oxford.

Data and materials availability:

All data associated with this study are present in the paper or supplementary materials. The microarray data generated by this study have been submitted to GEO depository under ID GSE109859.

Europe PMC Funders Author Manuscripts

Obesity is associated with changes in the secretome of adipose tissue (AT), which affects the vasculature through endocrine and paracrine mechanisms. Wingless-related integration site 5A (WNT5A) and secreted frizzled related protein 5 (SFRP5), adipokines that regulate non-canonical Wnt signaling, are dysregulated in obesity. We hypothesised that WNT5A released from AT exerts endocrine and paracrine effects on the arterial wall through non-canonical RAC1-mediated Wnt signaling. In a cohort of 1,004 humans with atherosclerosis, obesity was associated with increased WNT5A bioavailability in the circulation and the AT, higher expression of WNT5A receptors Frizzled 2 and 5 in the human arterial wall, and increased vascular oxidative stress due to activation of NADPH oxidases. Plasma concentration of WNT5A was elevated in patients with coronary artery disease compared to matched controls and was independently associated with calcified coronary plaque progression. We further demonstrated that WNT5A induces arterial oxidative stress and redox-sensitive migration of vascular smooth muscle cells via Frizzled 2-mediated activation of a previously uncharacterised pathway involving the deubiquitinating enzyme ubiquitin-specific protease 17 (USP17) and the GTPase RAC1. Our study identifies WNT5A and its downstream vascular signaling as a link between obesity and vascular disease pathogenesis, with translational implications in humans.

Introduction

Evidence suggests that obesity is closely related to vascular disease (1). However, the described U-shaped association between body mass index (BMI) and mortality(2) indicates the need for better understanding of the links between adipose tissue (AT) biology and vascular (patho)physiology in order to develop therapeutic strategies to prevent the vascular complications of obesity.

AT is a dynamic organ with regional biological variability (3), secreting a wide range of adipocytokines with vascular effects (4, 5). Perivascular AT (PVAT) exerts paracrine effects on the vascular wall, whereas “remote” AT depots such as subcutaneous (ScAT) and thoracic AT (ThAT) exert endocrine effects by enriching the circulating adipocytokine pool. Recent evidence suggests that obesity is associated with a shift of the AT secretome from vasoprotective/anti-atherogenic to a pro-atherogenic phenotype (6).

Redox signaling is central to vascular disease, exerting multiple cytotoxic and pro-inflammatory effects (7). NADPH oxidases (NOX) are major sources of vascular reactive oxygen species (ROS), and the activity of some NOX isoforms (namely NOX 1 and NOX 2) is dependent on the GTPase RAC1(8). In turn, ROS regulate the migration of vascular smooth muscle cells (VSMCs) to the intima layer of the vascular wall, which is involved in vascular disease processes such as atherosclerotic plaque formation (9). However, the mechanisms by which obesity affects vascular redox signaling are unclear.

The wingless-related integration site (Wnt) signaling pathway is activated by a family of Wnt glycoprotein ligands consisting of 19 members in humans (10) and is negatively regulated by secreted frizzled related proteins (Sfrp), which act as decoy receptors for Wnt ligands (11). Downstream Wnt signaling is mediated by the canonical pathway, which involves β-catenin and is triggered by WNT3 (10), and the non-canonical pathways, which do not involve β-catenin and are triggered by WNT5A and WNT11(12, 13). Despite the

established role of non-canonical Wnt signaling in cancer biology, its role in vascular disease pathogenesis in the context of obesity is unknown.

Recent work suggests that AT secretes WNT5A and SFRP5(14), molecules with potential vascular effects (15). Imbalance in the AT production of WNT5A and SFRP5 in obesity may result in a 'vicious cycle' of increased AT inflammation and insulin resistance (14), indirectly triggering vascular complications of obesity. However, the potential role of AT-derived WNT5A and SFRP5as direct mediators of atherogenesis in obesity has not been investigated so far. We hypothesised that dysregulated AT secretion of WNT5A and SFRP5may lead to altered endocrine and paracrine effects on the vascular wall in obesity. We further explored the potential links between AT-derived WNT5A and the mechanisms of vascular disease pathogenesis.

Results

Wnt ligand expression profile in adipose tissue depots from patients with atherosclerosis

We first explored the gene expression profile of all 19 Wnt ligands in human PVAT, ThAT and ScAT. *WNT5A* was the most highly expressed Wnt ligand in PVAT (Fig. 1A), whereas *WNT11* was the most highly expressed Wnt ligand in ThAT and ScAT, with *WNT5A* still being among the four most highly expressed Wnt ligands in these depots (Fig. 1, B and C). As both WNT5A and WNT11 are known to be non-canonical Wnt signaling pathway activators, and considering that WNT5A is the most abundant PVAT-derived paracrine ligand of the two, we focused on the potential role of WNT5A as a mediator of the vascular complications of obesity via non-canonical Wnt signaling.

WNT5A and SFRP5 adipose gene expression profiles in obesity

Plasma WNT5A was significantly increased in obese humans (Fig. 1D), accompanied by reduced plasma concentration of its antagonist SFRP5 (Figure 1E). We then focused on evaluating the WNT5A/SFRP5 ratio(16), since this is regarded as a more accurate integrated indication of overall Wnt signaling balance compared to evaluating WNT5A and SFRP5 concentrations individually. We observed a strong positive correlation between BMI and plasma WNT5A/SFRP5 ratio (Figure 1F). Consistently, there was a positive association between BMI and the gene expression of *WNT5A*/*SFRP5* in human ThAT (Fig. 1, G-I), but not in human ScAT (fig. S1, A-C). This suggests that increased *WNT5A*/*SFRP5* gene expression in visceral adiposity (ThAT) could be linked with obesity-related vascular disease in humans.

Interactions between obesity, WNT5A/SFRP5, and vascular disease

We next explored the associations between obesity, WNT5A/SFRP5, and markers of vascular disease. Although obesity was not associated with the gene expression of *WNT5A* (Fig. 2A), *SFRP5* (Fig. 2B), or the *WNT5A/SFRP5* ratio in human IMAs (Fig. 2C), it was linked with significantly altered gene expression of *WNT5A* and *SFRP5* in human PVAT. PVAT from obese/morbidly obese patients expressed significantly more *WNT5A* (Fig. 2D), less *SFRP5* (Fig. 2E), and thus had a higher *WNT5A/SFRP5* ratio compared to lean counterparts (Fig. 2F). Obesity was related to a significant increase in the gene expression of

WNT5A receptors Frizzled 2 (*FZD2*) (Fig. 2G) and Frizzled 5 (*FZD5*) (Fig. 2H) but not receptor tyrosine kinase-like orphan receptor 1 (*ROR1*) (Fig. 2I) in human IMAs. This suggests that, in obese humans, arteries display increased sensitivity to the consequences of Wnt signaling, which may be a mechanistic link to the increase in arterial oxidative stress observed in obesity.

To evaluate the association between the WNT5A/SFRP5 ratio and coronary artery disease (CAD) in humans, we designed a case-control study (study 2) in which 70 patients with CAD were matched for age, gender, and BMI with 70 controls without obstructive CAD [confirmed by computed tomography (CT) angiography as having no coronary plaque causing>50% luminal stenosis]. Patients with CAD had higher plasma WNT5A (Figure 2J), lower SFRP5 (Figure 2K), and a higher plasma WNT5A/SFRP5 ratio (Figure 2L) compared to controls. The presence of CAD was associated with circulating WNT5A (Bstand = 0.23, *P* = 0.00), SFRP5 (Bstand = -0.21, P = 0.00) and their ratio (Bstand = 0.21, P = 0.00) independently of traditional risk factors that differed significantly between the two cohorts of study 2 (Figure 2M). WNT5A/SFRP5 and all cardiovascular risk factors (hypertension, hyperlipidaemia, diabetes, and smoking) were associated with the presence of CAD by univariate analysis (table S1). However, in a multivariable model that included WNT5A/ SFRP5 and all risk factors, only hypertension and hyperlipidaemia remained independently associated with CAD, independently from each other (Fig. 2M).

To explore the potential value of WNT5A as a surrogate biomarker of vascular disease progression in humans, we designed a validation study (study 3) that involved individuals scanned by non-contrast CT at two different time points, 3-5 years apart, for evaluation of coronary calcified plaque burden. In 68 individuals studied, plasma WNT5A concentration was significantly elevated in patients that demonstrated calcified plaque progression, defined as a difference in coronary calcium score (CCS) ≥1 (n=32) (Figure 2N; baseline CCS: 0.00[0.00-76.70] and follow-up CCS: 15.63[0.00-182.88] presented as median [25th-75th percentile] in the entire study 3; differences in CCS between baseline and follow-up (ΔCSS) are further presented in Fig. 2N for each group)). Similarly, in 38 patients with baseline CCS=0, plasma WNT5A was positively associated with the development of new calcification (follow-up CCS: 0.00[0.00-6.93] presented as median [25th-75th percentile] in the entire study arm; follow-up CCS values in the new onset calcification group are also further presented in Fig. 2O). Upon multivariate regression analysis, plasma WNT5A was associated with progression of calcification (Bstand=0.242, P=0.047) and new onset calcification (Bstand=0.367, P=0.03) independently of age and sex (table S3).

WNT5A/SFRP5 as regulators of redox state in the human arterial wall

We observed that BMI was not only associated with increased circulating and AT WNT5A/ SFRP5 ratio but also with higher basal (Figure 3A) and NADPH-stimulated (Figure 3B) superoxide ($O_{2.}^-$) generation in human internal mammary artery (IMA) segments. To examine whether the WNT5A/SFRP5 balance could alter human arterial redox state and thus be a mechanistic link between obesity and oxidative stress, we next explored the interactions between $O_{2.}^-$ generation in human IMAs and WNT5A/SFRP5 ratio in plasma and PVAT from the patients in study 1. High plasma WNT5A/ SFRP5 ratio as well as high

WNT5A/ *SFRP5* expression in PVAT were related with higher basal and NADPH-stimulated $O_{2.}$- production in human IMAs (Figures 3C-F), whereas arterial *WNT5A*/*SFRP5* gene expression was not associated with arterial redox state (Figure 3G-H). Since endogenous *WNT5A* gene expression in the human IMA is negligible compared to that in PVAT (fig. S1D), we hypothesised that the effects of WNT5A on the arterial wall are endocrine (resulting from its increased concentration in the circulation and reaching the endothelium and VSMCs via the lumen and vasa vasorum for large arteries) and paracrine (reaching the VSMCs and the endothelium via diffusion from the PVAT) rather than autocrine.

To understand whether the association between obesity and NADPH oxidase activity in human arteries is dependent on the *WNT5A*/*SFRP5* ratio in PVAT, we performed multivariate analysis in which arterial NADPH-stimulated $O_{2.}$- was used as dependent variable, and obesity classification, diabetes, smoking, sex and age were used as independent variables. In the presence of *WNT5A*/*SFRP5* gene expression in PVAT, in the model, obesity was not a significant predictor of arterial NADPH-stimulated $O_{2.}$-, suggesting that the effects of obesity on human arterial redox state are WNT5A-dependent (table S4).

To explore whether the associations between WNT5A/SFRP5 and human vascular redox state are causal, we used *ex vivo* models of human IMAs (study 4), whereby serial IMA rings were incubated with WNT5A (100 ng/ml), SFRP5 (300 ng/ml), or the combination of the two factors for 45 minutes, and $O_{2.}$- generation was evaluated using lucigenin chemiluminescence and confirmed with dihydroethidium (DHE) staining. The concentration of WNT5A selected was near the maximum of the physiological amount of plasma WNT5A in patients of study 1 (range: 1-112 ng/ml). WNT5A induced a 4-fold increase in arterial basal $O_{2.}$-, an effect prevented by co-incubation with SFRP5 (Figure 3I). Similarly, NADPH-stimulated $O_{2.}$- was increased (>2-fold) by WNT5A incubation, an effect prevented by SFRP5 (Figure 3J), and the same was observed when measuring the signal inhibited by the pan-NOX inhibitor Vas2870 (Figure 3K).

The specificity of the signal and the structural $O_{2.}$- localization within the human arterial wall were examined using DHE staining of human IMAs. Incubation of human IMAs with WNT5A for 45 minutes increased $O_{2.}$- generation, mainly from the VSMCs layer, an effect partially attenuated by SFRP5 and completely reversed by Vas2870 (Figure 3L), confirming that the effect was dependent upon NADPH oxidases. To examine whether the consequences of WNT5A on vascular redox state are dependent on the activation of NADPH oxidases, we explored its effects on vascular $O_{2.}$- after pre-incubation of human arteries with Vas2870. In the presence of Vas2870, WNT5A failed to increase vascular $O_{2.}$-, confirming the central role of NADPH oxidases on the WNT5A -induced increase in vascular oxidative stress (Figure 3M-N). However, WNT5A did not affect the expression of any of the NOX isoforms (NOX1, NOX2, NOX4, or NOX5, fig. S2). In addition, plasma WNT5A/SFRP5 was not correlated with the expression of NOX2, NOX4, or NOX5 (fig. S3).

WNT5A also reduced nitric oxide (NO) bioavailability in human vessels [evaluated by ex vivo vasorelaxation in response to Acetylcholine (ACh)], an effect reversed by SFRP5 (fig. S4). WNT5A had no effect on the endothelium-independent responses to the NO donor sodium nitroprusside (SNP). To understand the underlying mechanism, we explored the

effect of WNT5A on endothelial nitric oxide synthase (eNOS) coupling. WNT5A induced eNOS uncoupling in human arteries, demonstrated by increased LNAME-inhibitable $O_{2.}$-, an effect reversed by SFRP5 (fig. S4). WNT5A promoted eNOS uncoupling by inducing the oxidation of eNOS co-factor tetrahydrobiopterin (BH4) without affecting the biopterin biosynthetic pathway (no modification of total vascular biopterin content, fig. S4). These data identify WNT5A as a regulator of vascular redox state that induces global changes in vascular redox signaling, influencing both VSMCs and the endothelium.

To further determine the causal effects of WNT5A on vascular NADPH oxidases activity in vivo, we used a doxycycline-inducible Tet-O- mouse model (*Wnt5a* +/*rtTA*+ mice) to induce global overexpression of *Wnt5a*. Treatment of *Wnt5a*+/*rtTA*+ mice with doxycycline induced marked overexpression of *Wnt5a* in multiple tissues (fig. S5) resulting in increased plasma WNT5A compared to doxycycline-treated *Wnt5a*–/*rtTA*+ littermate controls (Fig. 3O). *Wnt5a*+/*rtTA*+ mice demonstrated higher basal, NADPH-stimulated, and Vas2870-inhibitable aortic $O_{2.}$- generation (Fig. 3P-R) compared to *Wnt5a*–/*rtTA*+ controls, confirming that in vivo overexpression of WNT5A leads to activation of arterial NADPH oxidases.

Investigating the mechanism of WNT5A -induced arterial NADPH oxidases activation, we found that WNT5A activated the non-canonical planar cell polarity (PCP) Wnt signaling pathway, documented by c-Jun N-terminal kinase (JNK) phosphorylation (an established surrogate marker of PCP activation) in human IMAs as well as in the aortas of *Wnt5a*+/*rtTA* + mice (Fig. 4, A and B, respectively). WNT5A induced RAC1activation (Figure 4C) in human arteries, leading to membrane translocation of RAC1and P47phox subunits of NADPH oxidases (Fig. 4D and E), which are crucial for the activation of the NOX1 and NOX2 isoforms of NADPH oxidases. The key role of RAC1 in the WNT5A -mediated NADPH oxidases activation was shown by demonstrating that the specific RAC1inhibitor NSC23766 prevented the WNT5A -induced increase of basal, NADPH-stimulated, and Vas2870-inhibitable $O_{2.}$- in human IMAs (Figures 4F-H) and the aortas of *Wnt5a*+/*rtTA*+ mice (Fig. 4I-K).

Adipocyte-derived WNT5A as a paracrine regulator of redox state in human VSMCs

To explore whether adipocyte- derived WNT5A can exert paracrine effects that control the redox state in the neighboring VSMCs, we first confirmed that recombinant WNT5A activates the PCP pathway (JNK-phosphorylation) and activates RAC1in primary human VSMCs in culture (fig. S6, Fig. 5, A and B) similarly to intact vessels. We confirmed that a physiological concentration of WNT5A (100 ng/mL) did not activate the canonical Wnt signaling pathway (evaluated by quantifying active beta catenin), in contrast to supra-physiological WNT5A concentrations (400 ng/ml), which activated canonical Wnt signaling (Fig. 5C). Incubation with WNT5A (100 ng/mL) increased basal, NADPH-stimulated, and Vas2870-inhibitable $O_{2.}$- in VSMCs (Fig. 5D-F), suggesting that the effects observed at the level of whole vessel are largely driven by direct effects of WNT5A on VSMCs. We next used immortalized primary human preadipocytes endogenously expressing and secreting WNT5A and knocked down *WNT5A* using shRNA (Fig. 5G). We observed a significant reduction in basal VSMC $O_{2.}$- when VSMCs were co-cultured with WNT5A -knockout

(KO) adipocytes compared to sham control adipocytes (Fig. 5H). This reduction was due to a specific effect on the NOX2 isoform of NADPH oxidase in VSMCs, as confirmed by significant reduction in gp91-dstat-inhibitable $O_{2.}$- (gp91-dstat is a specific NOX2 inhibitor, Fig. 5I).

To further understand how WNT5A exerts its effects on human VSMCs in obesity, we knocked-down *FZD2* and *FZD5* (two receptors upregulated in arteries of obese humans) in VSMCs using siRNA (Fig. 6A-C). Down-regulation of *FZD2* was ~96%, and prevented the WNT5A -induced increase of basal, NADPH-stimulated, and Vas2870-inhibitable $O_{2.}$- in human VSMCs (Fig. 6D-F). Knocking down *FZD5* was less efficient in this model, with ~65% reduction of the gene expression in human VSMCs, and was related with a moderate reduction of the WNT5A-induced increase of basal (Fig. 6G) but not NADPH-stimulated (Fig. 6H) or Vas2870-inhibitable (Fig. 6I) $O_{2.}$- .

Effects of WNT5A on human VSMC migration

To better understand the cellular effects of WNT5A signaling on VSMC biology and the contribution of redox signaling in this context, we incubated human VSMCs with WNT5A (100 ng/ml) in the presence or absence of pegylated superoxide dismutase (peg-SOD, 100 IU/mL), a scavenger of $O_{2.}$-, and performed microarray analysis to evaluate the differential gene expression profile induced by WNT5A compared to non-treated controls. WNT5A altered the expression of 1,890 differentially expressed genes (DEGs), of which 1,057 genes were upregulated and 833 were down regulated (fig. S7A).

The protein products of a substantial number of these DEGs were implicated in signal transduction pathways controlling cell growth, cell division, cell death, cell fate, and cell motility (fig. S6B). Functional annotation using Gene Ontology (GO) database showed that 135 of these DEGs were involved in cell motility, acting through pathways known to regulate cell migration (Fig. 7, A-B). Thus, we hypothesised that WNT5A could influence the migration of primary human VSMCs.

We exposed human VSMCs to WNT5A (100 ng/ml) in the presence or absence of SFRP5 (300 ng/ml) and investigated changes in the ability of these cells to migrate using wound healing (fig. S7, C-D) and Boyden chamber (Fig. 7C) assays. WNT5A increased the migration of human VSMCs in a SFRP5-reversible manner (Fig. 7C-D), without affecting their proliferation (Fig. 7E). WNT5A could also induce a phenotypic switch of VSMCs, characterised by loss of contractile phenotype markers ACTA2 (actin α2, smooth muscle) and TGLN (trasngelin, or smooth muscle protein 22α, SM22α) and increased ratio of metalloproteinase 9 (MMP9) to MMP inhibitors TIMP1 and TIMP2 (fig. S8).

Ubiquitin-specific protease 17 (USP17) as a downstream regulator of WNT5A-mediated redox signaling

To determine the contribution of redox signaling to WNT5A-induced VSMC migration, we incubated primary human VSMCs with WNT5A in the presence or absence of peg-SOD. Peg-SOD prevented the WNT5A-induced changes in VSMC migration (Fig. 8A), suggesting that the changes in intracellular redox state described previously at least partially mediate the promigratory effects of WNT5A. Microarray results revealed that the effect of WNT5A

on 28 of the previously described migration-related DEGs was reversed (at least partly) by peg-SOD, highlighting the DEGs as potential redox-sensitive genes (Fig. 8B).

The maximally differentially regulated (upregulated) gene in response to WNT5A was USP17, a member of a deubiquitinating enzyme multigene family within a tandemly repeated sequence (17) (Figure 8B and fig. S9A). VSMCs isolated from 10 patients were subjected to in vitro WNT5A treatment with or without peg-SOD, and quantitative real time polymerase chain reaction (q-RT-PCR) confirmed that WNT5A increases the expression of USP17 (Figure 8C). USP17 was previously found to be involved in the activation of small GTPases (18) and to regulate cell motility (fig. S6).

To address the mechanistic role of USP17 in WNT5A-mediated RAC1activation, we knocked down USP17 using shRNA in HeLa cells (fig. S9B) and treated these cells with WNT5A (100ng/mL). WNT5A failed to induce persistent RAC1activation in USP17-KO HeLa cells as opposed to empty vector control cells (Fig. 8D). These data support the role of USP17 as a mediator of WNT5A-induced RAC1 activation and RAC1-mediated redox signaling, identifying a potential therapeutic target.

Discussion

We demonstrate that obesity leads to an imbalance between WNT5A and SFRP5expression in PVAT and other adipose tissue depots such as ThAT, as well as alterations in circulating plasma concentrations in human vascular disease. We show that obesity is associated with upregulation of WNT5A receptors Fzd2 and Fzd5, which are involved in non-canonical Wnt signaling in human arteries. WNT5A secreted by human adipocytes enhances arterial NADPH oxidases activity, increasing $O_{2.}$- generation and inducing endothelial dysfunction and eNOS uncoupling. This $O_{2.}$- excess (by both and NADPH oxidases and, secondarily, uncoupled eNOS) induces redox-driven migration in VSMCs via USP17/RAC1 activation, which may explain the clinical association of WNT5A with vascular disease. Patients with high plasma WNT5A were at higher risk for calcified plaque progression and new-onset coronary calcification. This work identifies WNT5A, its balance with SFRP5, and its receptors and downstream signaling network as mechanistic links between obesity and vascular complications in humans, and as a potential therapeutic target for the prevention and treatment of such complications.

AT tissue biology displays remarkable regional variability and is dysregulated in obesity (19). Several studies have documented the biological discrepancy between visceral and superficial AT (20) and identified inflamed visceral AT as a source of adipocytokines with detrimental paracrine and endocrine effects on the vasculature (5). Previous studies have shown that WNT5A is expressed in the human adipose tissue (21), and have suggested that the balance between WNT5A and its decoy inhibitor SFRP5 may be involved in the pathogenesis of obesity and diabetes (21). We hypothesised that WNT5A and SFRP5 secretion from dysfunctional adipose tissue could play a role in the development of vascular disease in obesity.

After observing that WNT5A was the most abundant Wnt ligand expressed in the human PVAT, we confirmed that obesity was associated high WNT5A and low SFRP5plasma concentrations in patients with CAD. We observed a similar shift of the *WNT5A/SFRP5* gene expression ratio in ThAT and PVAT surrounding the IMA. It is therefore likely that increased WNT5A release from these visceral AT depots -- as well as the overall increased mass of these adipose tissue depots in obesity -- contributes to the obesity-related increase in plasma WNT5A. Obesity not only increased the exposure of the human arteries to high circulating WNT5A/ low SFRP5 (inside-to-outside vascular effects, from the lumen to the vascular wall) and high *WNT5A* / low *SFRP5*from PVAT (outside-to-inside vascular effects, from PVAT to the vascular wall), but it also led to upregulation of WNT5A receptors Fzd2 and Fzd5 in the human arterial wall. These receptors increased arterial sensitivity to non-canonical Wnt signaling. The combination of increased plasma WNT5A, together with the increased release of WNT5A from PVAT, drives the endocrine and paracrine effects, respectively, of adipose tissue-derived WNT5A on the human vascular wall. In a second nested case-control study, we showed a striking increase of plasma WNT5A accompanied by reduced circulating Sfpr5 in patients with CAD compared to age, sex, and BMI matched non-CAD controls. Plasma WNT5A was positively and independently associated with both coronary calcification progression and new onset calcification in humans, suggesting that it has a clinically relevant role in vascular disease progression.

Previous reports have suggested that WNT5A may be involved in endothelial dysfunction, particularly in the context of diabetes (22, 23). These studies elegantly supported the notion that WNT5A signaling has vascular implications; however, the ability of WNT5A to regulate vascular redox state was unclear. Considering that obese individuals have elevated vascular oxidative stress due to activation of NADPH oxidases, we hypothesised that AT-derived WNT5A is a link between dysfunctional AT and vascular disease in obesity, and this could be mediated by its effects on human arterial redox state. Redox signaling is directly involved in multiple vascular diseases commonly presented as complications of obesity (24–26). NADPH oxidases comprise major sources of ROS in the human vascular wall (8). The activation of NOX1 and NOX2 isoforms of NADPH oxidases is dependent on the activation and membrane translocation of RAC1and $P47_{phox}$ cytoplasmic subunits in order to form the active enzymatic complex (27). Given that non-canonical Wnt signaling has been linked with activation of small GTPases like Rac, we hypothesised that adipose tissue-derived WNT5A may drive arterial oxidative stress via RAC1-mediated NADPH oxidases activation in obesity, as well as by eNOS uncoupling via BH4 oxidation.

Here we demonstrated that high WNT5A/SFRP5 ratio, either in plasma or in PVAT surrounding human arteries, is related to significantly higher $O_{2.}$- generation in these vessels. The causal association of WNT5A with human arterial $O_{2.}$- was subsequently confirmed using *ex vivo* models of human arteries, and the precise mechanisms were further elucidated *in vitro* using primary human VSMCs. The *in vivo* effects of WNT5A on vascular NADPH oxidases activity was then confirmed using a doxycycline-inducible tet-O- WNT5A model. WNT5A appears to trigger non-canonical Wnt signaling at low (physiological) concentrations, as confirmed in our work, whereas high, supra-physiological concentrations of WNT5A may trigger canonical Wnt signaling. The effect of physiological concentrations of WNT5A on cellular redox state in human VSMCs is mediated by Fzd2 receptor-induced

non-canonical activation of RAC1, resulting in the translocation of GTP-RAC1 and $P47_{phox}$ to the cell membrane and leading to enzymatic stimulation of NADPH oxidases in the vasculature. Co-culture of human adipocytes with human VSMCs revealed that knocking-down WNT5A in human pre-adipocytes results into a reduction of $O_{2.}$- generation by NOX2in VSMCs, confirming the paracrine role of adipocyte-derived WNT5A on vascular redox state.

The balance between VSMCs migration and proliferation versus apoptosis is crucial for the stability of atherosclerotic plaques (28). Migration of these cells is believed to contribute to atherogenesis, particularly at the early disease stage (29). VSMCs may undergo a phenotypic switch whereby they lose their contractile phenotype markers and start producing metalloproteinases which may lead to fibrous cap thinning a plaque rupture (28). Previous studies have linked WNT5A signaling to reduced VSMCs apoptosis (30), but this effect was attributed to canonical Wnt signaling achieved using a supra-physiological WNT5A concentration in vitro (30). Conversely, WNT5A stimulates cellular motility and migration via non-canonical signaling in a variety of cell types (31, 32), while oxidative stress can also promote the migration of VSMCs (9). In this context, we hypothesised that WNT5A may affect VSMC phenotype and specifically lead to VSMC migration at least partially via induction of redox signaling.

We demonstrated that WNT5A induces migration of human VSMCs in a redox-sensitive manner which is reversed by peg-SOD, a scavenger of intracellular $O_{2.}$- . WNT5A may cause a VSMC phenotypic switch, evidenced by downregulation of contractile gene markers *ACTA2* and *TAGLN* (28) and a concomitant increase in the bioavailability of MMP9, a metalloproteinase with strong associations with plaque rupture (33). Transcriptome analysis revealed that WNT5A regulates a number of migration-related genes in human VSMCs, thus potentially exerting multiple effects on VSMC migration. USP17, a deubiquitinating enzyme acting as a known activator of small GTPases like RAC (18), was the top hit up-regulated by WNT5A (and partly reversed by peg-SOD) in VSMCs. The USP17/ RAC1 link has previously been implicated in diseases in which cell motility plays a pivotal role, such as tumorigenesis (34). However, USP17 has not previously been implicated in vascular biology, nor has it been proposed as a downstream target of WNT5A signaling. Our data supports a role for USP17 in mediating the effects of WNT5A on RAC1activation and controlling vascular redox state, while the link between WNT5A and USP17 also appears to be partly redox-sensitive. These data identify the WNT5A/USP17/RAC1/NADPH oxidases axis as a potential therapeutic target to modify the vascular effects of obesity.

A limitation of the current study is the lack of *in vivo* mechanistic data linking WNT5A overexpression with atherosclerosis. Although we demonstrated that high plasma concentrations of WNT5A were related to faster progression of coronary atherosclerosis and development of new coronary calcified plaques in humans, an *in vivo* experimental model would potentially prove causality of this association. Further, prospectively designed, clinical studies are required to determine the prognostic value of circulating WNT5A as a biomarker for the prediction of vascular disease related outcomes (e.g., calcified plaque progression, clinical endpoints such as non-fatal myocardial infarction, stroke, cardiac mortality). Finally it remains unclear whether WNT5A secretion from the adipose tissue

Europe PMC Funders Author Manuscripts

and/or WNT5A-reated vascular signalling could be targeted therapeutically, and whether such an intervention would have the potential to prevent the vascular complications of obesity.

Obesity is associated with enhanced activation of non-canonical Wnt signaling in the human arterial wall resulting from a shift in the balance between WNT5A and SFRP5 both in the circulation and in PVAT and up-regulation of the WNT5A receptors Fzd2 and 5 on the arterial wall. This results in USP17-mediated activation of RAC1 and downstream activation of vascular NADPH oxidases, leading to $O_{2.}^-$ -induced migration of VSMCs. At a clinical level, WNT5A concentration is independently associated with the presence of CAD and progression of calcified coronary atherosclerotic plaque burden. These data identify UPS17 and WNT5A as rational targets for the prevention and /or treatment of vascular complications associated with obesity in humans.

Methods

Study design

The aim of this work was to explore the role of AT-derived WNT5A in regulating vascular redox signalling and vascular disease progression in humans. We hypothesised that WNT5A would be upregulated in obesity and would be able to induce vascular NADPH oxidase activation via RAC1 signalling, which could have downstream redox signalling effects triggering vascular disease.

To address these hypotheses, we first explored the associations between obesity, arterial $O_{2.}^-$ generation and the bioavailability of WNT5A in the circulation and a variety of AT depots (ScAT, ThAT, PVAT) in a cohort of 1,004 patients undergoing cardiac surgery (study 1, see below). These were used to provide observational insights as to the relationship of WNT5A with arterial oxidative stress in the context of obesity. Power size calculations for these clinical studies indicated that we would need 933 patients to detect a 10% difference in arterial NADPH-stimulated $O_{2.}^-$ between the low and high plasma WNT5A/SFRP5 tertile with $\alpha = 0.05$ and power of 0.90 assuming an SD of 100 RLU/sec/mg tissue.

The clinical link of circulating WNT5A with parameters of vascular disease (presence of CAD, calcified plaque progression, new onset calcification) was tested in a validation study of 70 CAD patients matched with 70 non-CAD controls (study 2, see below) and a follow-up study of CCS monitoring in patients having undergone two cardiac CT scans, where baseline and follow-up CCS scores were evaluated and circulating WNT5A was quantified. With 70 patients per group, we could detect a difference of 10ng/mL in plasma WNT5A with $\alpha = 0.05$ and power 0.9 (assuming plasma WNT5A SD = 9ng/mL).

Ex vivo mechanistic experiments were employed to test the direct signalling effects of WNT5A incubations on human arteries harvested during surgery, in a series of mechanistic experiments performed in a paired design for individuals patients. Based on previous work from our group, we estimated that with a minimum of 5 pairs of samples (serial rings from the same vessel) we would be able to identify a change of $\log(O_{2.}^-)$ by 0.48 with $\alpha = 0.05$, power 0.9 and SD for a difference in the response of the pairs of 0.25.

The effect of WNT5A on arterial $O_{2.}$- production was validated with a short-term proof-of-concept mouse experiment of global inducible *Wnt5a* overexpression upon doxycycline treatment. We estimated that with 5 mice per group we could detect a difference of 250 RLU/sec/mg tissue in aortic $O_{2.}$- with $\alpha = 0.05$ and power 0.9 assuming an aortic NADPH-stimulated $O_{2.}$- SD of 120 RLU/sec/mg tissue).

The integrated effects of WNT5A on vascular redox state and downstream redox signalling events such as cell migration were evaluated in vitro in primary VSMCs isolated from human vascular segments. Similarly to the ex vivo experiments, we estimated that with 5 pairs of wells we would be able to identify a change of 175 RLU/sec/μg protein in VSMC NADPH- stimulated $O_{2.}$- with α=0.05, power 0.9 and SD = 85 RLU/sec/μg protein.

Human study protocols were in agreement with the Declaration of Helsinki and all patients provided written informed consent prior to enrolment. All studies (clinical or experimental) were performed blinded. Human studies were approved by local research ethics committees (under RECs 11/SC/0140 and 15/SC/0545). All animal studies were conducted with ethical approval from the Local Ethical Review Committee and in accordance with the UK Home Office regulations (Guidance on the Operation of Animals, Scientific Procedures Act, 1986).

Human studies protocols

Study protocols were in agreement with the Declaration of Helsinki and all patients provided written informed consent prior to enrolment. The demographic characteristics of the participants of all study arms are presented in table S1. Hyperlipidaemia and hypertension were defined according to the latest European Society Cardiology Guidelines (35, 36). Diabetes mellitus was defined according to the American Diabetes Association guidelines (37). Obesity was defined according to the Adult Treatment Panel (ATP) III guidelines (38).

In vivo clinical studies (studies 1-3)—Study 1 comprised 1,004 prospectively enrolled patients undergoing cardiac surgery [including coronary artery bypass grafting (CABG) and valve replacement/repair] at the John Radcliffe hospital, Oxford University NHS Foundation Trust, UK. Exclusion criteria included inflammatory, neoplastic, renal, or hepatic diseases. Fasting blood samples were obtained on the morning of surgery and were used for plasma isolation for circulating biomarker measurements. During surgery, segments of the IMA with its surrounding PVAT, ThAT from the paracardial region, and ScAT from the chest were collected, transferred to the lab on ice, and processed for ex vivo experiments, vasomotor studies, and measurement of vascular $O_{2.}$- . Study 2 included 70 individuals with CAD and 70 controls without CAD (confirmed with coronary CT angiography). Individuals were matched for age, gender, and BMI for cross-sectional studies comparing circulating WNT5A and SFRP5. Study 3 consisted of 68 individuals that underwent two non-contrast CT scans 3-5 years apart (48.5±5.8 months), to study progression of atherosclerotic disease in the coronary arteries. The development of new calcification and the progression of existing calcified atherosclerotic plaques were compared between the two scans.

Ex vivo studies with human vessels (study 4)—The human ex vivo study (study 4) included 94 patients undergoing cardiac surgery at the John Radcliffe hospital, Oxford University NHS Foundation Trust, UK. Patients were prospectively recruited and patients

with inflammatory, neoplastic, renal or hepatic diseases were excluded. Human IMA and saphenous vein (SV) segments were collected during surgery and transferred to the lab on ice. IMA samples were processed in the lab as explained in relevant sections, subjected to *ex vivo* incubations and ultimately used for vascular O_{2}.- quantification, vasomotor studies, biopterin measurements and downstream signaling evaluation as described later.

In vivo animal studies

A doxycycline-inducible WNT5A knock-in mouse model was used to determine the *in vivo* effects of WNT5A on vascular NADPH oxidases activity. FVB/N Tg(tetO- *Wnt5a*)17Rva/J mice were obtained from Jackson Laboratories (stock #022938), and crossed to mixed background C57BL/6, 129/SV, FVB CAGG-*rtTA* (generated by Dr. Lukas Dow in the lab of Dr. Scott Lowe at Memorial Sloan Kettering Cancer Centre, USA) (39). Mice were backcrossed to C57BL/6 background seven times prior to the study. TetO-W*nt5a*+ and *rtTA* + mice were then crossed obtaining double transgenic mice, *rtTA*+ single transgenic mice were kept as control animals. 2mg/mL doxycycline hyclate (J60579, Alfa Aesar) was administered, to both double transgenic tetO- *Wnt5a*+/*rtTA*+ and control tetO-*Wnt5a*–/rtTA + animals via the drinking water, containing 5% sucrose overnight to induce *Wnt5a* expression. Considerable weight loss (up to ~15% of body weight) was observed after three days of doxycycline treatment, therefore this mouse model was not suitable for long-term experiments as per local committee ethics. Overnight doxycycline treatment induced minor weight loss and did not compromise the welfare of the animals. DNA extracted from experimental animal ear notches was used for genotyping with the following PCR primers:

C57BL/6, FVB CAG-*rtTA*

CCM 5’- CGAAACTCTGGTTGACATG - 3’

CTG 5’- ATGCCCTGGCTCACAAATAC - 3’

CWT 5’- TGCCTATCATGTTGTCAAA – 3’

C57BL/6, FVB/N Tg(tetO- *Wnt5a*)17Rva/J

17815 5’- ACAAAGACGATGACGACAAGC – 3’

17816 5’- CGCACCTTCTCCAATGTACTG – 3’

oIMR7338 5’- CTAGGCCACAGAATTGAAAGATCT – 3’

oIMR7339 5’ – GTAGGTGGAAATTCTAGCATCATCC – 3’

Mice were housed in a specific pathogen-free environment, in Tecniplast Sealsafe IVC cages (floor area 542 cm_{2}) with a maximum of six other mice. Mice were kept in a 12 h light/dark cycle and in controlled temperatures (20–22°C) and fed normal chow and water ad libitum. A detailed phenotyping of the mouse model is presented in fig. S4.

Europe PMC Funders Author Manuscripts

Blood Sampling and Circulating Biomarker Measurements

Humans—Preoperative venous blood samples were collected from subjects of Study 1 after 8h of fasting and in particular on the morning of surgery as previously described (40). Blood samples were also collected from subjects of Study 2 after 8h of fasting upon admission. Similarly, blood samples from Study 3 participants were collected after 8h of fasting just prior to the cardiac CT scans. After centrifugation at 2000 g at 4°C for 15 min, plasma was collected and stored at −80 °C until assayed. Plasma WNT5A and SFRP5 were measured by using commercially available ELISA kits (Cloud Clone Corp, catalogue number SEP549Hu and MyBiosource, catalogue number MBS702373 respectively) following the manufacturer's instructions.

Mice—900 μl blood was drawn from the vena cava into a syringe containing sodium heparin. Blood samples were centrifuged for 15 minutes at 3,000 rpm at room temperature. Plasma was subsequently centrifuged for 5 minutes at 13,000 rpm to remove remaining cells and platelets and immediately frozen at -80°C. Plasma WNT5A was measured by using a commercially available ELISA kit (Cloud Clone Corp, catalogue number SEP549Mu) following the manufacturer's instructions.

Human Adipose Tissue and Vessel Harvesting

Internal mammary artery (IMA) samples were harvested with a "no touch" technique with their perivascular tissue (PVAT) at the time of CABG as we have described previously (42). Vascular segments were transferred into oxygenated (95% O2/5% CO_2) ice-cold Krebs Hensleit buffer and the vessel lumen was flushed gently by using an insulin syringe to remove blood. Each vessel was separated from its surrounding adipose tissue in the lab, under magnification by the same operator, to limit the between-patients variability. The same anaesthetics were used in all cases, and each sample was always obtained at the same stage of the operation, to limit inter-patient variability. ThAT and ScAT specimens were collected during surgery, then snap-frozen in TRI reagent (Sigma, catalogue number T9424) and stored at -80oC until used for RNA isolation.

Transcriptome profiling of WNT5A-treated VSMCs

Treatments and RNA extraction—VSMCs isolated from five individual patients were incubated 8 hours with 100 ng/mL WNT5A or 100 U/mL peg-SOD. Patients were selected to be obese and without diabetes mellitus, allowing us to evaluate the integrated effects of WNT5A in the clinically relevant setting of obesity. RNA was extracted from VSMCs using the MagMAX mirVana total RNA isolation kit (Thermo Fischer Scientific, Catalogue Number A27828) as mentioned earlier, and processed for high throughput gene expression profiling.

GeneChip human transcriptome array 2.1—The genome-wide expression profiling was carried out at the High Throughput Genomics Wellcome Trust Centre for Human Genetics (Oxford, UK). RNA samples were processed using the Affymetrix GeneChip WT PLUS Reagent kit, the manual target preparation for GeneChip whole transcript expression arrays. The labelled ss-cDNA were then hybridised to the Affymetrix HuGene-2.1-st Array

Plate and processed on the Affymetrix GeneTitan platform. The microarray data generated by this study have been submitted to GEO depository under ID GSE109859.

Statistical analysis

Continuous variables were tested for normal distribution using the Kolmogorov-Smirnov test. Non-normally distributed variables are presented as median [25_{th}-75th percentile] and whiskers (Tukey). Normally distributed variables are presented as mean±SEM. Comparisons of continuous variables between two groups were performed using unpaired t test or Man-Whitney U-test as appropriate, while comparisons between 3 or more groups were performed using one-way ANOVA or Kruskal-Wallis followed by Bonferroni or Dunn's post hoc correction for multiple comparisons. Paired comparisons were performed using paired t test or Wilcoxon signed-rank test as appropriate. For between-groups serial changes we used two-way ANOVA for repeated measures with interaction terms as presented in the figure legends.

To examine whether the association between obesity and vascular NADPH oxidase activity is independent of *WNT5A*/*SFRP5* expression in PVAT, we performed multivariate linear regression where NADPH-stimulated $O_{2.}$- was used as dependent variable and obesity classification, age, sex, diabetes, hypertension and smoking (with/without the addition of *WNT5A*/*SFRP5* expression tertiles in PVAT) were used as independent variables. The relevant standardised beta coefficients are presented. To address whether plasma WNT5A, SFRP5 and the ratio of the two were independently associated with the presence of CAD in the nested case-control study 2, we performed multivariate linear egression in which the presence of CAD was used as dependent variable and hypertension, hyperlipidaemia, smoking and plasma WNT5A or SFRP5or WNT5A/SFRP5 ratio were used as independent variables. The standardized beta (Bstand) is presented for each variable. To examine whether coronary calcified plaque progression or new onset calcification were associated with plasma WNT5A, we performed multivariate linear regression where calcified plaque progression and new onset calcification were used as dependent variables and plasma WNT5A, age and sex were used as independent variables. All statistical tests were two-tailed and were performed using SPSS version 20.0. $P < 0.05$ was considered statistically significant. Individual subject-level data are provided in data file S1.

With regards to microarray data processing, normalisation, quality control and differential gene expression analysis was performed with the Affymetrix Transcriptome Analysis Console (TAC 4.0) Software. The statistical comparisons between treatments was done following a repeated measures model for the individual patients. WNT5A pathway enrichment analysis was carried out in ConsensusPathDB-human with differentially expressed genes (DEGs) (WNT5A -treated vs. untreated-controls) that displayed fold change (linear)>1 or <-1 and a p-value (condition pair)< 0.05. Gene Ontology database was used to functionally annotate DEGs.

Supplementary Material

Refer to Web version on PubMed Central for supplementary material.

Acknowledgments

We would like to thank Prof C. W. Pugh for providing the rtTA mouse strain and the Oxford High Throughput Genomics Centre for contributing to microarray experiments.

Funding

This study was supported by the British Heart Foundation (FS/16/15/32047 and PG/13/56/30383 to CA, CH/16/1/32013 to KC, and Centre of Research Excellence award RG/13/1/30181), the National Institute for Health Research Oxford Biomedical Research Centre, the European commission (ITN network RADOX) and the NovoNordisk Foundation (NNF15CC0018486). I.A. acknowledges support by the Alexandros S. Onassis Public Benefit Foundation. We thank the High-Throughput Genomics Group at The Wellcome Trust Centre for Human Genetics (funded by Wellcome Trust grant reference 090532/Z/09/Z) for the generation of the microarray data. A.P.C. is supported by a Novo Nordisk Postdoctoral Fellowship run in partnership with the University of Oxford. C.C. acknowledges support by the British Heart Foundation (FS/16/45/32359).

References

1. Bastien M, Poirier P, Lemieux I, Despres JP. Overview of epidemiology and contribution of obesity to cardiovascular disease. Prog Cardiovasc Dis. 2014; 56:369–381. [PubMed: 24438728]
2. Aune D, Sen A, Prasad M, Norat T, Janszky I, Tonstad S, Romundstad P, Vatten LJ. BMI and all cause mortality: systematic review and non-linear dose-response meta-analysis of 230 cohort studies with 3.74 million deaths among 30.3 million participants. BMJ. 2016; 353
3. Arner P, Backdahl J, Hemmingsson P, Stenvinkel P, Eriksson-Hogling D, Naslund E, Thorell A, Andersson DP, Caidahl K, Ryden M. Regional variations in the relationship between arterial stiffness and adipocyte volume or number in obese subjects. Int J Obes (Lond). 2015; 39:222–227. [PubMed: 25002147]
4. Akoumianakis I, Tarun A, Antoniades A. Perivascular adipose tissue as a regulator of vascular disease pathogenesis: identifying novel therapeutic targets. Br J Pharmacol. 2017; 174:3411–3424. [PubMed: 27976387]
5. Fuster JJ, Ouchi N, Gokce N, Walsh K. Obesity-Induced Changes in Adipose Tissue Microenvironment and Their Impact on Cardiovascular Disease. Circ Res. 2016; 118:1786–1807. [PubMed: 27230642]
6. Oikonomou EK, Antoniades C. Immunometabolic Regulation of Vascular Redox State: The Role of Adipose Tissue. Antioxid Redox Signal. 2017
7. Li H, Horke S, Forstermann U. Vascular oxidative stress, nitric oxide and atherosclerosis. Atherosclerosis. 2014; 237:208–219. [PubMed: 25244505]
8. Konior A, Schramm A, Czesnikiewicz-Guzik M, Guzik TJ. NADPH oxidases in vascular pathology. Antioxid Redox Signal. 2014; 20:2794–2814. [PubMed: 24180474]
9. Papaharalambus CA, Griendling KK. Basic mechanisms of oxidative stress and reactive oxygen species in cardiovascular injury. Trends Cardiovasc Med. 2007; 17:48–54. [PubMed: 17292046]
10. Kikuchi A, Yamamoto H, Sato A. Selective activation mechanisms of Wnt signaling pathways. Trends Cell Biol. 2009; 19:119–129. [PubMed: 19208479]
11. Kawano Y, Kypta R. Secreted antagonists of the Wnt signaling pathway. J Cell Sci. 2003; 116:2627–2634. [PubMed: 12775774]
12. Veeman MT, Axelrod JD, Moon RT. A second canon. Functions and mechanisms of beta-catenin-independent Wnt signaling. Dev Cell. 2003; 5:367–377. [PubMed: 12967557]
13. Reis M, Liebner S. Wnt signaling in the vasculature. Exp Cell Res. 2013; 319:1317–1323. [PubMed: 23291327]
14. Ouchi N, Higuchi A, Ohashi K, Oshima Y, Gokce N, Shibata R, Akasaki Y, Shimono A, Walsh K. SFRP5 is an anti-inflammatory adipokine that modulates metabolic dysfunction in obesity. Science. 2010; 329:454–457. [PubMed: 20558665]
15. Ackers I, Szymanski C, Duckett KJ, Consitt LA, Silver MJ, Malgor R. Blocking WNT5A signaling decreases CD36 expression and foam cell formation in atherosclerosis. Cardiovasc Pathol. 2018; 34:1–8. [PubMed: 29474941]

16. Schulte DM, Muller N, Neumann K, Oberhauser F, Faust M, Gudelhofer H, Brandt B, Krone W, Laudes M. Pro-inflammatory WNT5A and anti-inflammatory SFRP5 are differentially regulated by nutritional factors in obese human subjects. PLoS One. 2012; 7:e32437. [PubMed: 22384249]
17. Burrows JF, McGrattan MJ, Johnston JA. The DUB/USP17 deubiquitinating enzymes, a multigene family within a tandemly repeated sequence. Genomics. 2005; 85:524–529. [PubMed: 15780755]
18. de la Vega M, Kelvin AA, Dunican DJ, McFarlane C, Burrows JF, Jaworski J, Stevenson NJ, Dib K, Rappoport JZ, Scott CJ, Long A, et al. The deubiquitinating enzyme USP17 is essential for GTPase subcellular localization and cell motility. Nat Commun. 2011; 2
19. Akoumianakis I, Antoniades C. The interplay between adipose tissue and the cardiovascular system: is fat always bad? Cardiovasc Res. 2017; 113:999–1008. [PubMed: 28582523]
20. Alexopoulos N, Katritsis D, Raggi P. Visceral adipose tissue as a source of inflammation and promoter of atherosclerosis. Atherosclerosis. 2014; 233:104–112. [PubMed: 24529130]
21. Catalan V, Gomez-Ambrosi J, Rodriguez A, Perez-Hernandez AI, Gurbindo J, Ramirez B, Mendez-Gimenez L, Rotellar F, Valenti V, Moncada R, Marti P, et al. Activation of noncanonical Wnt signaling through WNT5A in visceral adipose tissue of obese subjects is related to inflammation. J Clin Endocrinol Metab. 2014; 99:E1407–1417. [PubMed: 24840810]
22. Farb MG, Karki S, Park SY, Saggese SM, Carmine B, Hess DT, Apovian C, Fetterman JL, Breton-Romero R, Hamburg NM, Fuster JJ, et al. WNT5A-JNK regulation of vascular insulin resistance in human obesity. Vasc Med. 2016; 21:489–496. [PubMed: 27688298]
23. Breton-Romero R, Feng B, Holbrook M, Farb MG, Fetterman JL, Linder EA, Berk BD, Masaki N, Weisbrod RM, Inagaki E, Gokce N, et al. Endothelial Dysfunction in Human Diabetes Is Mediated by WNT5A-JNK Signaling. Arterioscler Thromb Vasc Biol. 2016; 36:561–569. [PubMed: 26800561]
24. Keaney JF, Larson MG, Vasan RS, Wilson PW, Lipinska I, Corey D, Massaro JM, Sutherland P, Vita JA, Benjamin EJ, Framingham S. Obesity and systemic oxidative stress: clinical correlates of oxidative stress in the Framingham Study. Arterioscler Thromb Vasc Biol. 2003; 23:434–439. [PubMed: 12615693]
25. Ceriello A, Motz E. Is oxidative stress the pathogenic mechanism underlying insulin resistance, diabetes, and cardiovascular disease? The common soil hypothesis revisited. Arterioscler Thromb Vasc Biol. 2004; 24:816–823. [PubMed: 14976002]
26. Akoumianakis I, Antoniades C. Impaired Vascular Redox Signaling in the Vascular Complications of Obesity and Diabetes Mellitus. Antioxid Redox Signal. 2018
27. Guzik TJ, Harrison DG. Vascular NADPH oxidases as drug targets for novel antioxidant strategies. Drug Discov Today. 2006; 11:524–533. [PubMed: 16713904]
28. Bennett MR, Sinha S, Owens GK. Vascular Smooth Muscle Cells in Atherosclerosis. Circ Res. 2016; 118:692–702. [PubMed: 26892967]
29. Chappell J, Harman JL, Narasimhan VM, Yu H, Foote K, Simons BD, Bennett MR, Jorgensen HF. Extensive Proliferation of a Subset of Differentiated, yet Plastic, Medial Vascular Smooth Muscle Cells Contributes to Neointimal Formation in Mouse Injury and Atherosclerosis Models. Circ Res. 2016; 119:1313–1323. [PubMed: 27682618]
30. Mill C, Monk BA, Williams H, Simmonds SJ, Jeremy JY, Johnson JL, George SJ. WNT5A-induced Wnt1-inducible secreted protein-1 suppresses vascular smooth muscle cell apoptosis induced by oxidative stress. Arterioscler Thromb Vasc Biol. 2014; 34:2449–2456. [PubMed: 25212236]
31. Hasan MK, Yu J, Chen L, Cui B, WidhopfIi GF, Rassenti L, Shen Z, Briggs SP, Kipps TJ. WNT5A induces ROR1 to complex with HS1 to enhance migration of chronic lymphocytic leukemia cells. Leukemia. 2017; 31:2615–2622. [PubMed: 28465529]
32. Kikuchi A, Yamamoto H, Sato A, Matsumoto S. WNT5A: its signaling, functions and implication in diseases. Acta Physiol (Oxf). 2012; 204:17–33. [PubMed: 21518267]
33. Yabluchanskiy A, Ma Y, Iyer RP, Hall ME, Lindsey ML. Matrix metalloproteinase-9: Many shades of function in cardiovascular disease. Physiology (Bethesda). 2013; 28:391–403. [PubMed: 24186934]

34. McFarlane C, Kelvin AA, de la Vega M, Govender U, Scott CJ, Burrows JF, Johnston JA. The deubiquitinating enzyme USP17 is highly expressed in tumor biopsies, is cell cycle regulated, and is required for G1-S progression. Cancer Res. 2101; 70:3329–3339.
35. Catapano AL, Graham I, De Backer G, Wiklund O, Chapman MJ, Drexel H, Hoes AW, Jennings CS, Landmesser U, Pedersen TR, Reiner Z, et al. 2016 ESC/EAS Guidelines for the Management of Dyslipidaemias. Eur Heart J. 2016; 37:2999–3058. [PubMed: 27567407]
36. Mancia G, Fagard R, Narkiewicz K, Redon J, Zanchetti A, Bohm M, Christiaens T, Cifkova R, De Backer G, Dominiczak A, Galderisi M, et al. 2013 ESH/ESC guidelines for the management of arterial hypertension: the Task Force for the Management of Arterial Hypertension of the European Society of Hypertension (ESH) and of the European Society of Cardiology (ESC). Eur Heart J. 2013; 34:2159–2219. [PubMed: 23771844]
37. Garza L, Dols J, Gillespie M. An initiative to improve primary prevention of cardiovascular disease in adults with type II diabetes based on the ACC/AHA (2013) and ADA (2016) guidelines. J Am Assoc Nurse Pract. 2017; 29:606–611. [PubMed: 28772017]
38. E. National Cholesterol Education Program Expert Panel on Detection, A. Treatment of High Blood Cholesterol in, Third Report of the National Cholesterol Education Program (NCEP) Expert Panel on Detection, Evaluation, and Treatment of High Blood Cholesterol in Adults (Adult Treatment Panel III) final report. Circulation. 2002; 106:3143–3421. [PubMed: 12485966]
39. Premsrirut PK, Dow LE, Kim SY, Camiolo M, Malone CD, Miething C, Scuoppo C, Zuber J, Dickins RA, Kogan SC, et al. A rapid and scalable system for studying gene function in mice using conditional RNA interference. Cell. 2011; 145:145–158. [PubMed: 21458673]
40. Antonopoulos AS, Margaritis M, Coutinho P, Shirodaria C, Psarros C, Herdman L, Sanna F, De Silva R, Petrou M, Sayeed R, Krasopoulos G, et al. Adiponectin as a link between type 2 diabetes and vascular NADPH oxidase activity in the human arterial wall: the regulatory role of perivascular adipose tissue. Diabetes. 2015; 64:2207–2219. [PubMed: 25552596]
41. Agatston AS, Janowitz WR, Hildner FJ, Zusmer NR, Viamonte M, Detrano R. Quantification of coronary artery calcium using ultrafast computed tomography. J Am Coll Cardiol. 1990; 15:827–832. [PubMed: 2407762]
42. Antoniades C, Shirodaria C, Warrick N, Cai S, de Bono J, Lee J, Leeson P, Neubauer S, Ratnatunga C, Pillai R, Refsum H, et al. 5-methyltetrahydrofolate rapidly improves endothelial function and decreases superoxide production in human vessels: effects on vascular tetrahydrobiopterin availability and endothelial nitric oxide synthase coupling. Circulation. 2006; 114:1193–1201. [PubMed: 16940192]
43. Margaritis M, Antonopoulos AS, Digby J, Lee R, Reilly S, Coutinho P, Shirodaria C, Sayeed R, Petrou M, De Silva R, Jalilzadeh S, et al. Antoniades, Interactions between vascular wall and perivascular adipose tissue reveal novel roles for adiponectin in the regulation of endothelial nitric oxide synthase function in human vessels. Circulation. 2013; 127:2209–2221. [PubMed: 23625959]
44. Antoniades C, Shirodaria C, Crabtree M, Rinze R, Alp N, Cunnington C, Diesch J, Tousoulis D, Stefanadis C, Leeson P, Ratnatunga C, et al. Altered plasma versus vascular biopterins in human atherosclerosis reveal relationships between endothelial nitric oxide synthase coupling, endothelial function and inflammation. Circulation. 2007; 116:2851–2859. [PubMed: 18040031]
45. Antoniades C, Bakogiannis C, Leeson P, Guzik TJ, Zhang MH, Tousoulis D, Antonopoulos AS, Demosthenous M, Marinou K, Hale A, Paschalis A, et al. Rapid, direct effects of statin treatment on arterial redox state and nitric oxide bioavailability in human atherosclerosis via tetrahydrobiopterin-mediated entohelial nitric oxide synthase coupling. Circulation. 2011; 124:335–345. [PubMed: 21730307]
46. Pfaffl MW. A new mathematical model for relative quantification in real-time RT-PCR. Nucleic Acids Res. 2001; 29:e45. [PubMed: 11328886]
47. Todorcevic M, Hilton C, McNeil C, Christodoulides C, Hodson L, Karpe F, Pinnick KE. A cellular model for the investigation of depot specific human adipocyte biology. Adipocyte. 2017; 6:40–55. [PubMed: 28452592]

Europe PMC Funders Author Manuscripts

One sentence summary

Adipose-secreted WNT5A triggers vascular disease in obesity, activating vascular smooth muscle cell migration by an NADPH oxidase-dependent mechanism.

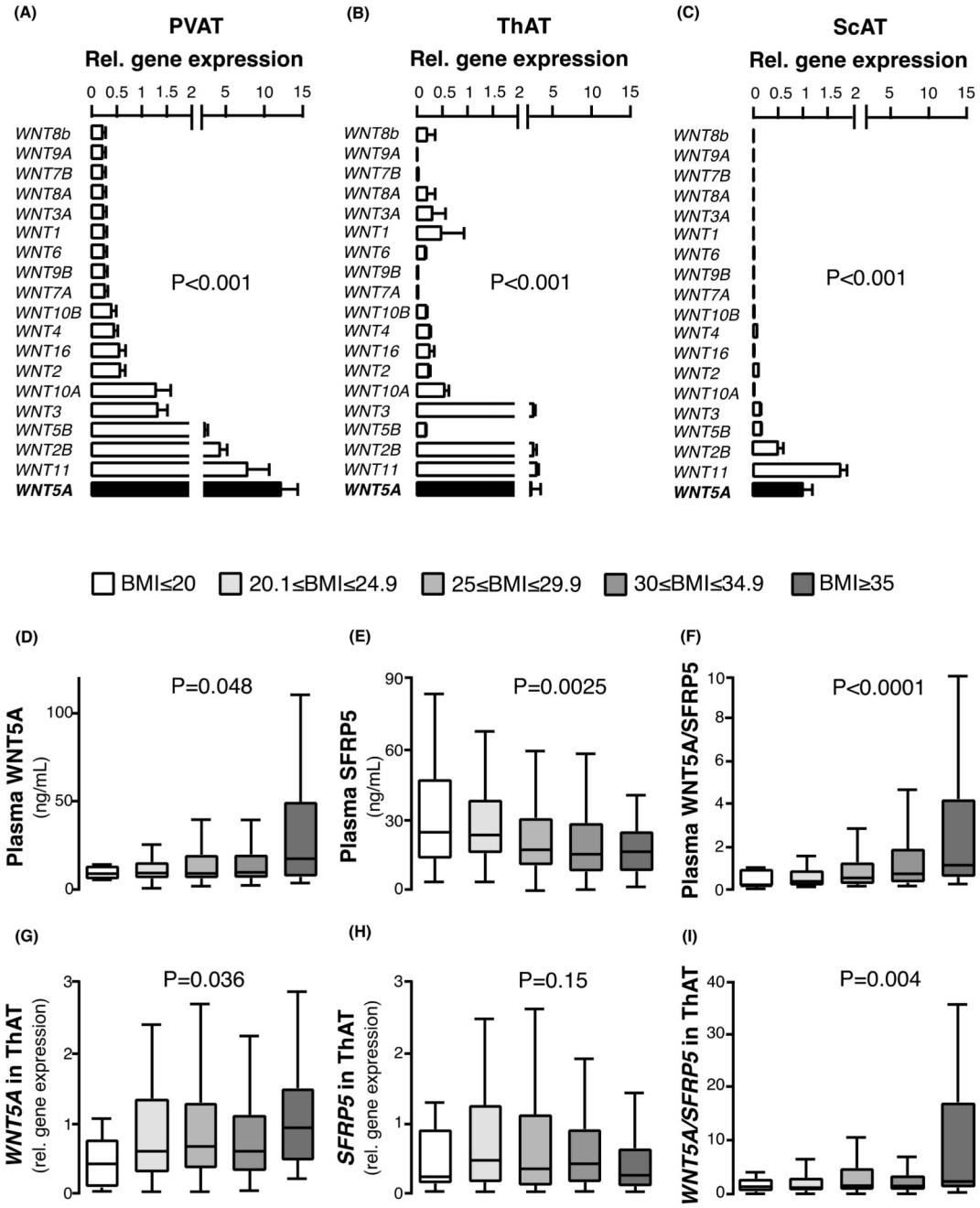

Fig. 1. Gene expression of Wnt ligands in adipose tissue and plasma concentration of WNT5A/SFRP5 in obesity.

(**A**-**C**) Gene expression of the 19 Wnt ligands in human (A) perivascular (PVAT), (B) thoracic (ThAT), and (C) subcutaneous (ScAT) AT in $n = 54$ patients of study 1. (**D**-**F**) Circulating plasma concentrations of (D) WNT5A (range: 1 to 112 ng/ml), (E) decoy receptor SFRP5, and (F) WNT5A/SFRP5 ratio in individuals of study 1. (**G**-**I**) Gene expression of (G) *WNT5A*, (B) *SFRP5*, and (C) the ratio of *WNT5A/SFRP5* in ThAT of study 1 participants. Study 1 participants per group: BMI: ≤20Kg/m_2: 25; 20.1-24.9 Kg/m_2:

217; 25-29.9 Kg/m_2: 432; 30-34.9 Kg/m_2: 233; ≥35 Kg/m_2: 57. Data are presented as mean ± SEM (A-C) or median [25_{th}-75_{th} percentile] (D-I). *P* values in (A-C) are calculated by Friedman tests; *P* values in (D-I) are calculated by Kruskal Wallis tests. AT: adipose tissue; SEM: Standard error of the mean.

Europe PMC Funders Author Manuscripts

Europe PMC Funders Author Manuscripts

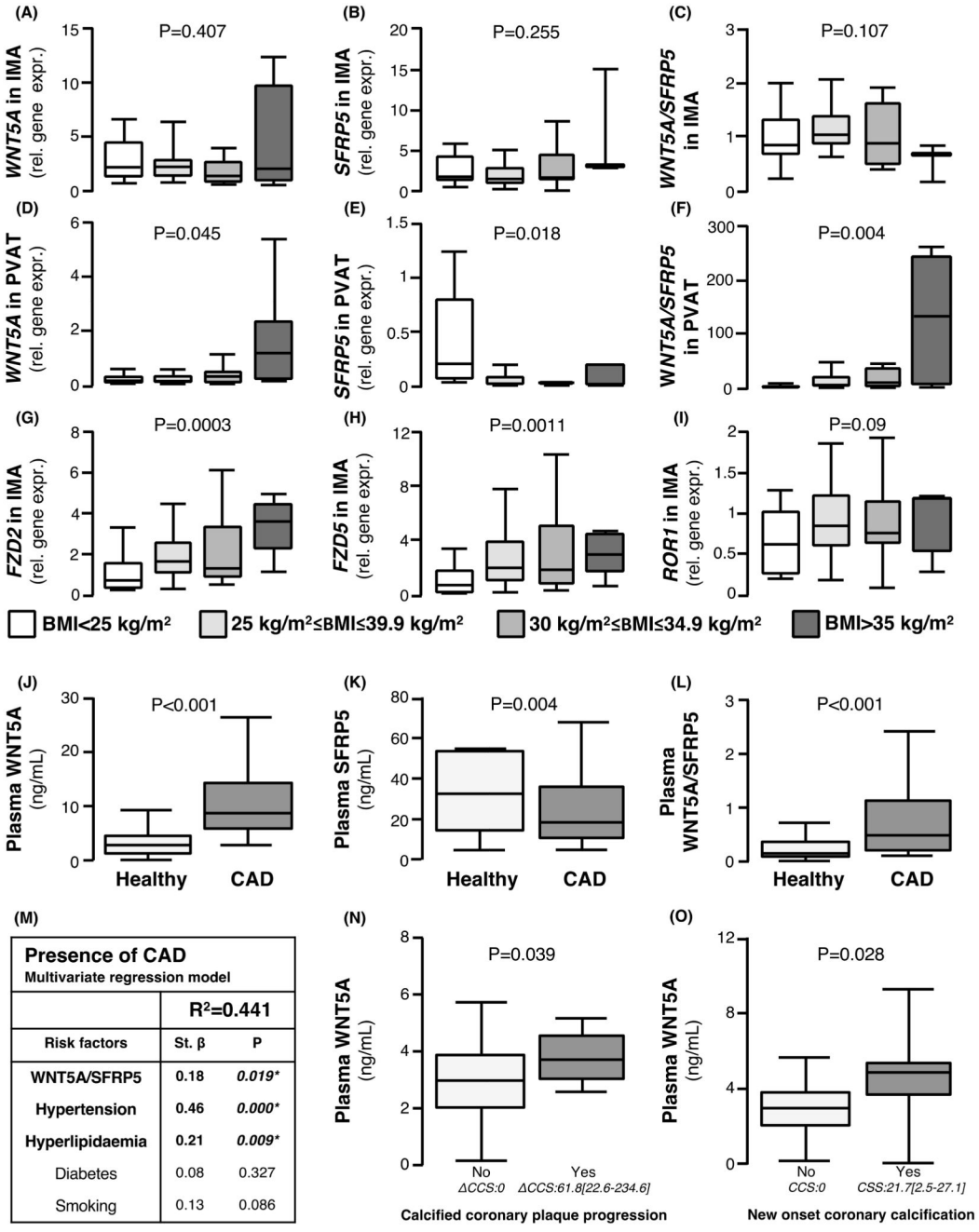

Fig. 2. Interactions between obesity, WNT5A/SFRP5, and vascular disease.

(**A**-**C**) Gene expression of (A) *WNT5A*, (B) *SFRP5*, and (C) the ratio of *WNT5A/SFRP5* in IMAs according to BMI. (**D**-**F**) Gene expression of (D) *WNT5A*, (E) *SFRP5*, and (C) the ratio of *WNT5A/SFRP5* in PVAT according to BMI. (**G**-**I**) Gene expression of Wnt receptors (G) *FZD2*, (H) *FZD5*, and (I) *ROR1* in IMAs according to BMI. (**J**-**L**) Circulating plasma concentrations of (J) WNT5A, (K) SFRP5, and (L) WNT5A/SFRP5 ratio in patients with CAD and healthy controls ($n = 70$). (**M**) Table of multivariable regression analysis of the association of circulating WNT5A, SFRP5, WNT5A/SFRP5, cardiovascular risk factors,

and the presence of CAD in study 2 (n = 70). (**N**) Plasma WNT5A concentration in patients with or without coronary calcium score (CCS) progression (ΔCCS≥1HU, 61.8 [22.6-234.6], n = 68, study 3). (**O**) Plasma WNT5A concentration in patients with or without new onset calcification (follow-up CSS:21.7[2.5-27.1], n=38). (N-O) presented as median [25_{th}-75_{th} percentile]. Data are presented as median [25_{th}-75_{th} percentile]. P values in (A-N) are calculated by Kruskal Wallis tests. Study 1 participants with IMA/PVAT samples available for panels A-I were: BMI<25Kg/m_2: 33; 25-29.9Kg/m_2: 77; 30-30Kg/m_2:42; >35 Kg/m_2:13. IMA: internal mammary artery; BMI: body mass index; PVAT: perivascular adipose tissue; CAD: coronary artery disease.

Europe PMC Funders Author Manuscripts

Europe PMC Funders Author Manuscripts

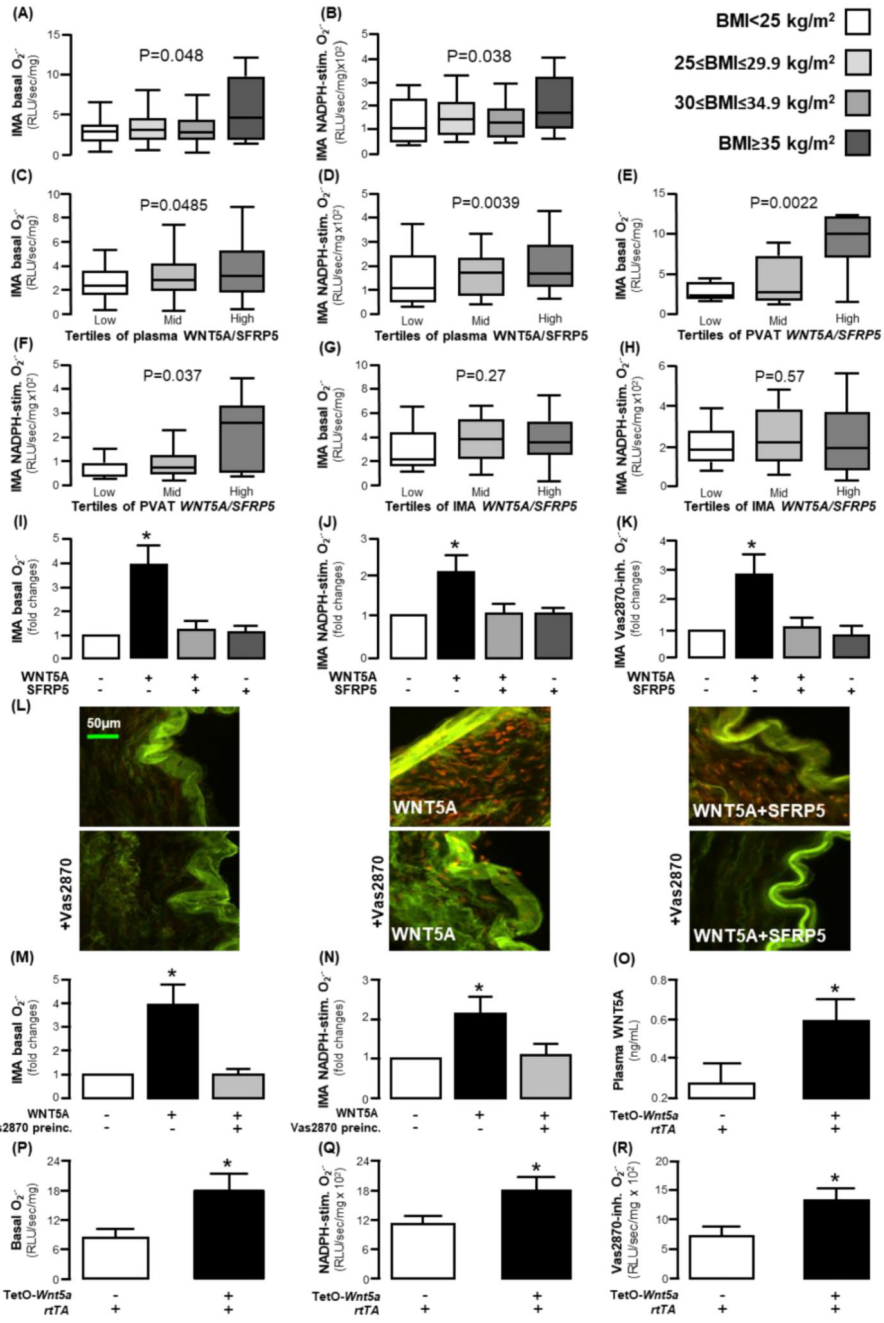

Fig. 3. WNT5A regulates vascular redox state in humans.

(**A**) Basal and (**B**) NADPH-stimulated superoxide ($O_{2.}$-) production in internal mammary artery (IMA) segments according to BMI (study 1). (**C**) Basal and (**D**) NADPH-stimulated $O_{2.}$- production in IMAs according to circulating plasma WNT5A/SFRP5 ratio tertiles. (**E**) Basal and (**F**) NADPH-stimulated $O_{2.}$- production in IMAs according to *WNT5A/SFRP5* ratio tertiles in perivascular adipose tissue (PVAT). (**G**) Basal and (**H**) NADPH-stimulated $O_{2.}$- production in IMAs according to *WNT5A/SFRP5* ratio tertiles in internal mammary arteries (IMAs). (**I**) Basal, (**J**) NADPH-stimulated, and (**K**) Vas2870-inhibitable $O_{2.}$-

production in IMAs in the presence and absence of WNT5A and SFRP5 in ex vivo IMA segments (n =5-10 pairs per intervention). (**L**) Dihydorethidium (DHE) staining in IMAs incubated with or without Vas2870, WNT5A, and SFRP5 (specific oxidised DHE fluorescence corresponds to the red signal; the green signal reflects tissue autofluorescence). (**M**) Basal or (**N**) NADPH-stimulated $O_{2.}$- production in IMAs in pre-incubated (preinc.) with Vas2870 and treated with WNT5A (n = 5-10 pairs per intervention). (**O**) Circulating plasma WNT5A (n = 11-14 mice per group) and (**P**) basal $O_{2.}$-, (**Q**) NADPH-stimulated $O_{2.}$-, and (**R**) Vas2870-inhibitable $O_{2.}$- in TetOWNT5A mouse aortae (O: n = 5 per group, P-R: n = 7 per group). Data are presented as median [25_{th}-75_{th} percentile] (A-H) or as mean ± SEM (I-K, N-R). P values in (A-H) are calculated by Kruskal Wallis tests; *P < 0.05 vs control in (I-J) and (M-N) by Wilcoxon signed-rank tests; P values are calculated by Mann Whitney U tests in (O-R).

Europe PMC Funders Author Manuscripts

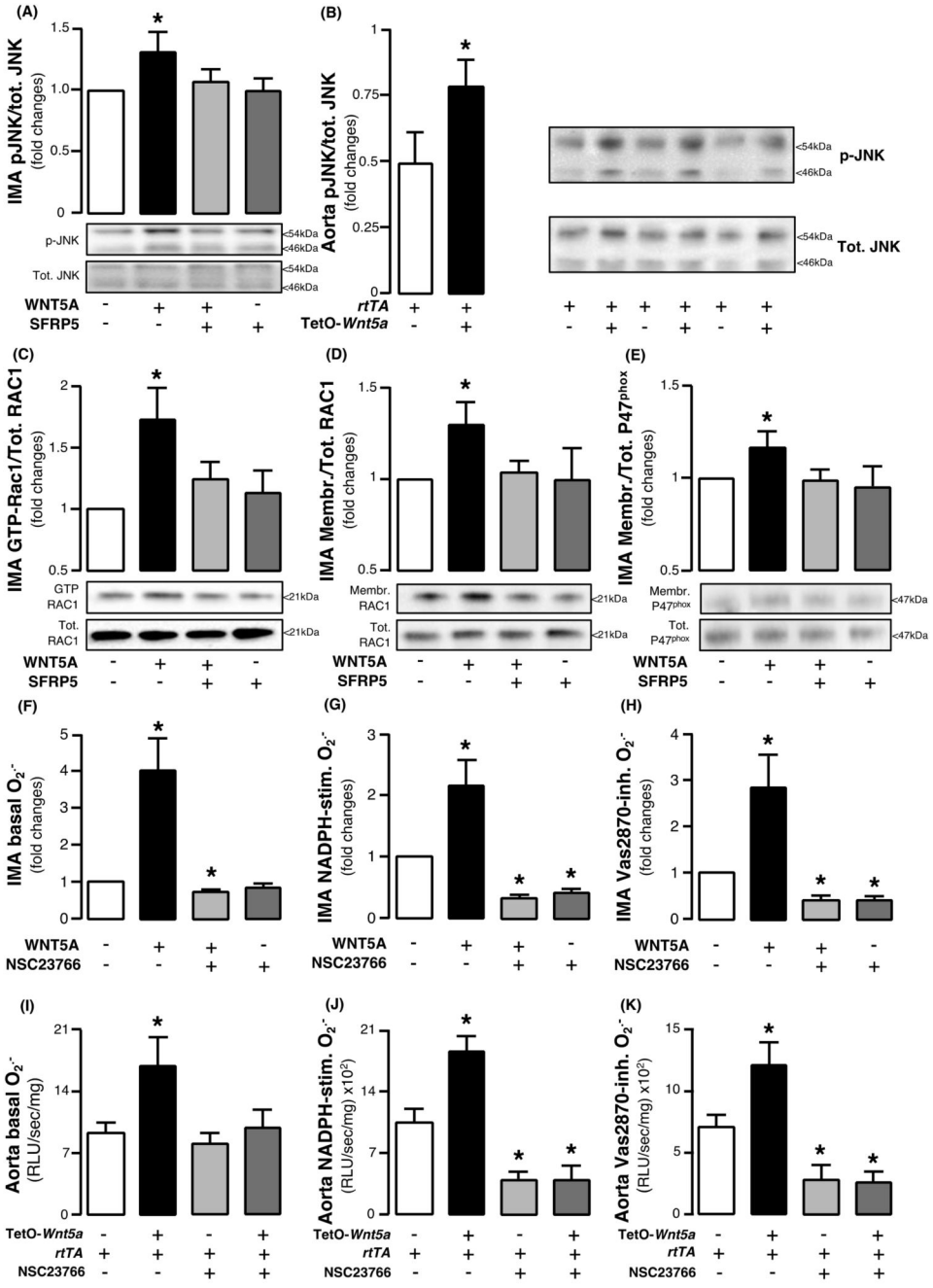

Fig. 4. WNT5A triggers RAC1activation, resulting in NADPH oxidases in the human vascular wall.

Fold change of phosphorylated c-jun N-terminal kinase (JNK) in (**A**) human internal mammary artery (IMA) segments ex vivo (n=5 of paired samples) in the presence and absence of WNT5A and SFRP5 and in (**B**) *Wnt5a*+/*rtTA*+ mouse aortae in vivo (n = 5 per group. (**C**) Activation of RAC1 and membrane translocation of (**D**) RAC1 and (**E**) P47phox subunits of NADPH oxidases in human IMAs (n = 5 of paired samples) ex vivo in the presence or absence of WNT5A and SFRP5. (**F**) Basal, (**G**) NADPH-stimulated, and (**H**)

Vas2870-inhibitable superoxide ($O_{2.}^-$) anion production in IMA segments with or without WNT5A and NSC23766, a specific RAC1 inhibitor (n = 8-10 pairs per intervention). (**I**) Basal, (**J**) NADPH-stimulated, and (**K**) Vas2870-inhibitable superoxide ($O_{2.}^-$) anion production in *Wnt5a*+/*rtTA*+ mouse aortae incubated with or without WNT5A and NSC23766 (n = 5-7 per group). Data are presented as mean ± SEM.*P > 0.05 vs control in all panels by Wilcoxon signed rank tests. SEM: Standard error of the mean.

Europe PMC Funders Author Manuscripts

Europe PMC Funders Author Manuscripts

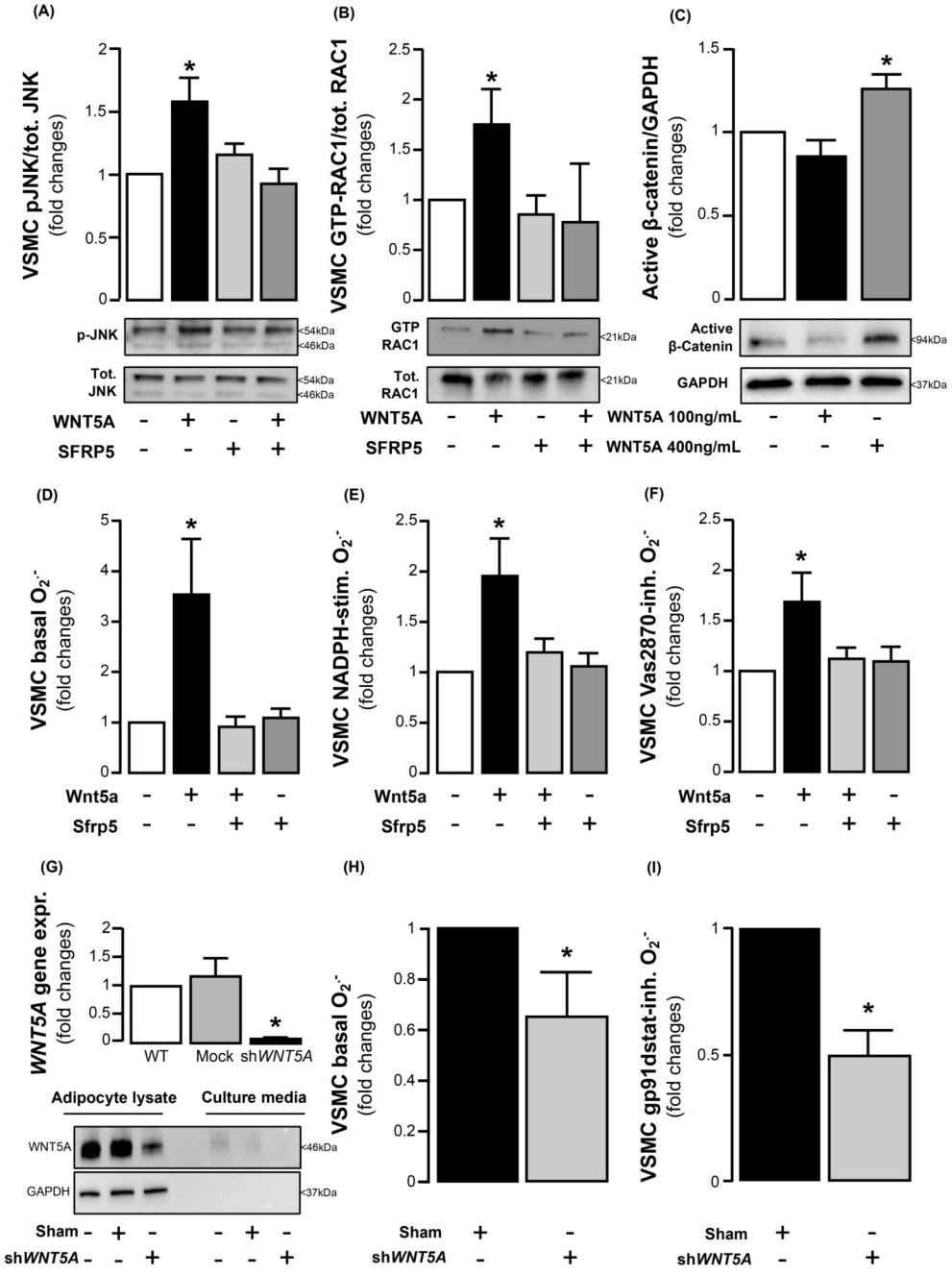

Fig. 5. WNT5A is secreted by adipocytes and enhances NADPH oxidase activity in human vascular smooth muscle cells via RAC1 activation.

Fold change of (**A**) phosphorylated c-Jun N-terminal kinase (JNK) ($n = 5$), (**B**) activated RAC1 ($n = 5$), and (**C**) activated β-catenin ($n = 6$) in VSMCs in the presence or absence of WNT5A and SFRP5. (**D**) Basal, (**E**) NADPH-stimulated, and (**F**) Vas2870-inhibitable superoxide ($O_{2\cdot}^-$) production in VSMCs ($n = 6$-11 pairs per intervention) in the presence or absence of WNT5A and SFRP5. (**G**) Knock-down of *WNT5A* in human immortalised pre-adipocytes ($n = 3$). (**H**) Basal and (**I**) gp91 dstat-inhibitable $O_{2\cdot}^-$ production in VSMCs co-

cultured with or without *WNT5A* -KO preadipocytes displayed lower ($n = 5$). Data are presented as mean ± SEM $^{*}P < 0.05$ vs control by Wilcoxon signed ranks tests (A-F, H-I) or paired t-test (G). SEM: Standard error of the mean.

Europe PMC Funders Author Manuscripts

Europe PMC Funders Author Manuscripts

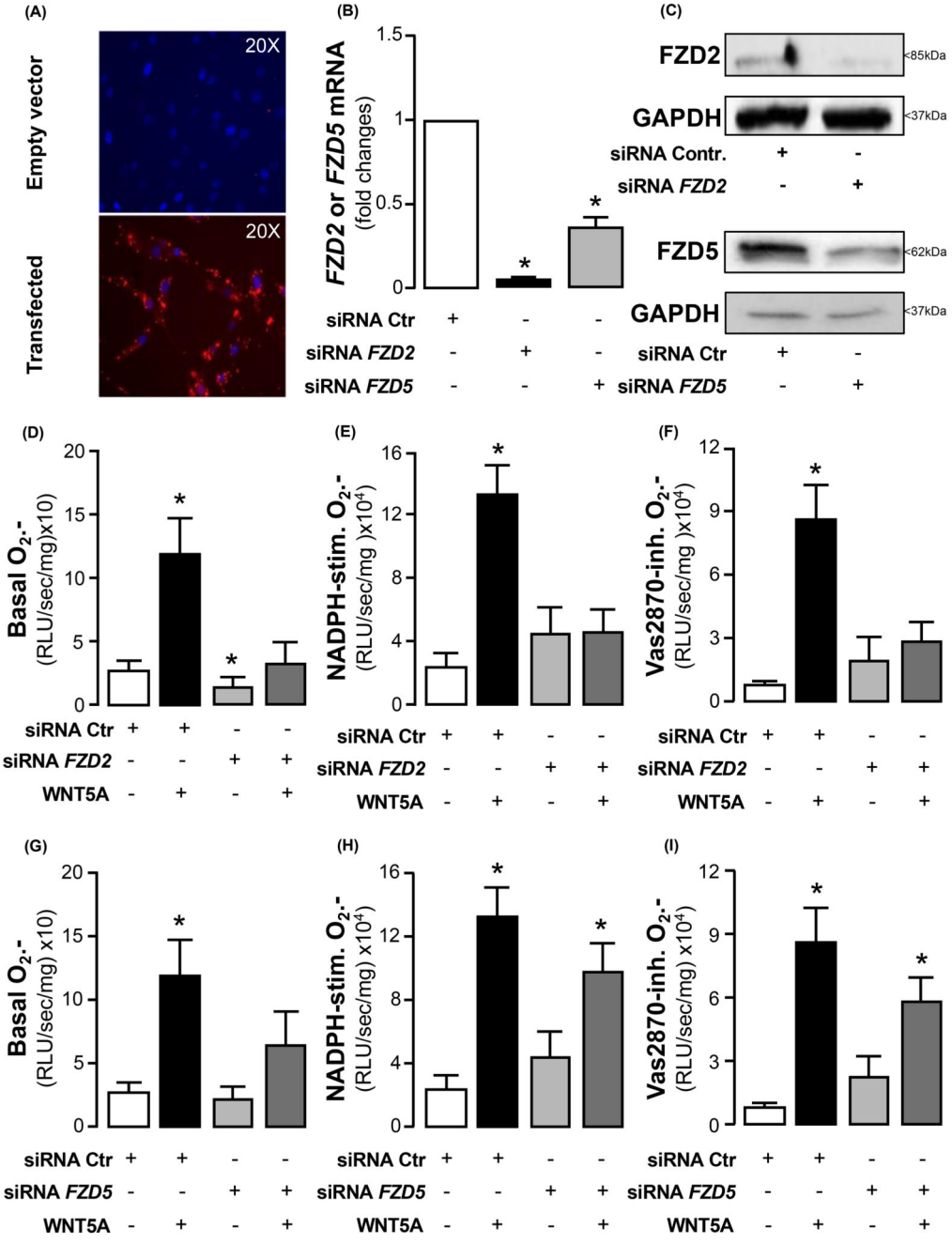

Fig. 6. The pro-oxidant effects of WNT5A in human vascular smooth muscle cells are mediated by Frizzled 2 (Fzd2) and Frizzled 5 (Fzd5) receptors.

(**A**) Fluorescence lipofectamine RNAimax imaging (BLOCK-iT Alexa Fluor Red Fluorescence) against cell nuclei stained with DAPI (blue signal), (**B**) fexpression old change, and (**C**) Western blotting of transfection efficiency of knock-down of *FZD2* and *FZD5* genes in VSMCs (~96% downregulation of *FZD2*, ~65% downregulation of *FZD5; n* = 3). (**D**) Basal, (**E**) NADPH-stimulated, and (**F**) Vas2870-inhibitable $O_{2.}$- production in siRNA-*FZD2*-treated VSMCs (*n* = 5-6 pairs per intervention) in the presence or absence of

WNT5A. (**G**) Basal, (**H**) NADPH-stimulated, and (**I**) Vas2870-inhibitable $O_{2.}$- production in siRNA-*FZD5*-treated VSMCs (n = 6 pairs per intervention) in the presence or absence of WNT5A. Data are presented as mean ± SEM. *P < 0.05 vs control by Wilcoxon signed ranks tests (D-I) or paired t-test (B). SEM: Standard error of the mean.

Europe PMC Funders Author Manuscripts

Europe PMC Funders Author Manuscripts

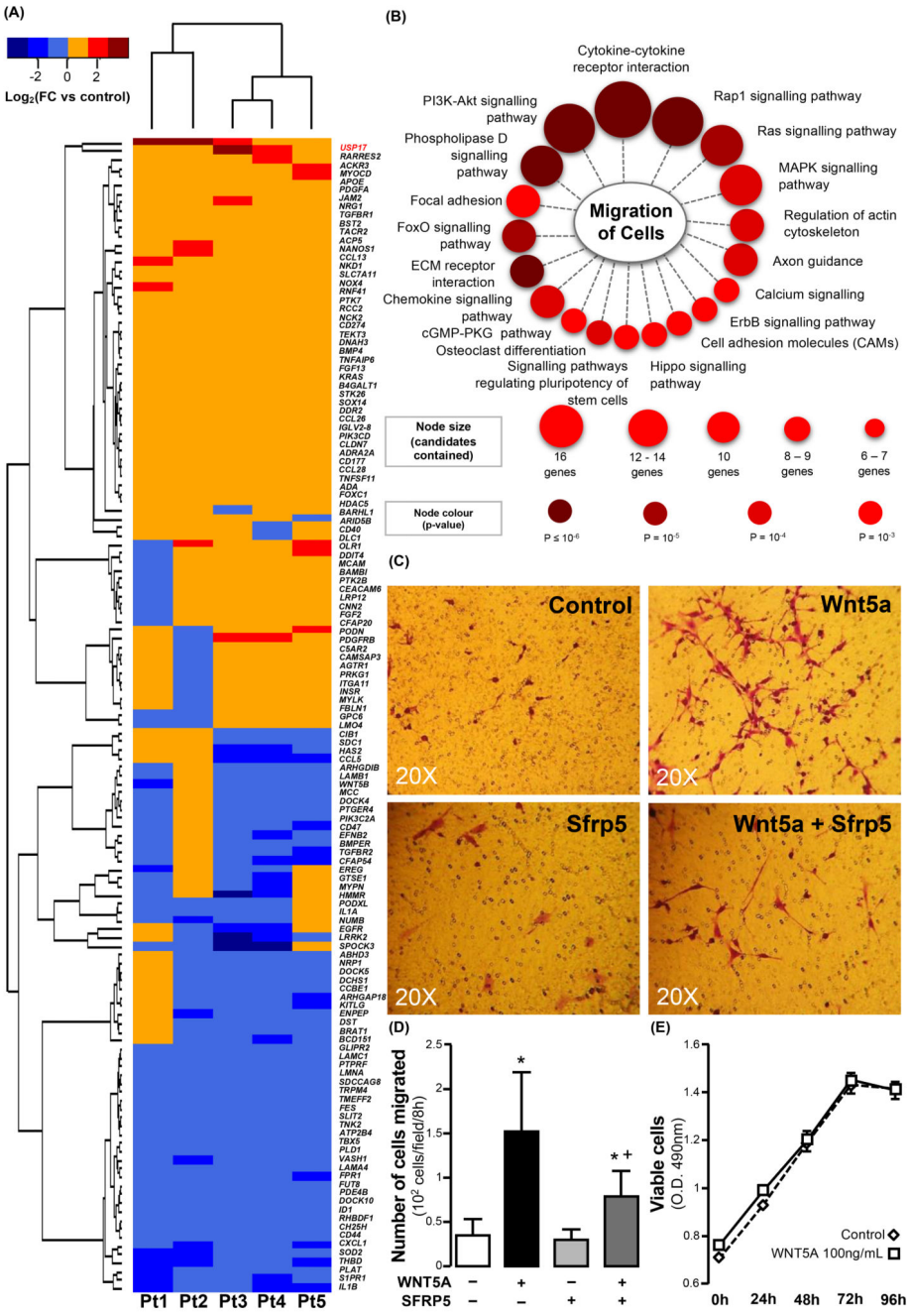

Fig. 7. WNT5A triggers redox-dependent migration of human vascular smooth muscle cells.

(**A**) Hierarchical clustering of 136 WNT5A differentially expressed genes (DEGs, Fold change > 1 or < -1, $P \leq 0.05$) in WNT5A -treated VSMCs from $n = 5$ patients. DEGs were annotated with cell motility function in Gene Ontology (GO) database. (**B**) Enriched signaling pathways of WNT5A cell-motility DEGs identified through ConsensusPathDB. (**C**) Microscopy and (**D**) quantitation of Boyden chamber assay for cell migration, using VSMCs treated with or without recombinant WNT5A and SFRP5 ($n = 30$). (**E**) Proliferation of VSMCs in the presence of WNT5A ($n = 6$-9 per time point per group, evaluated by two-

way ANOVA for repeated measures). Data are presented as mean ± SEM in panels D-E. *P < 0.05 vs control by Wilcoxon signed rank tests; +P < 0.05 vs WNT5A by Wilcoxon signed rank test. SEM: Standard error of the mean; FC: Fold change.

Europe PMC Funders Author Manuscripts

Europe PMC Funders Author Manuscripts

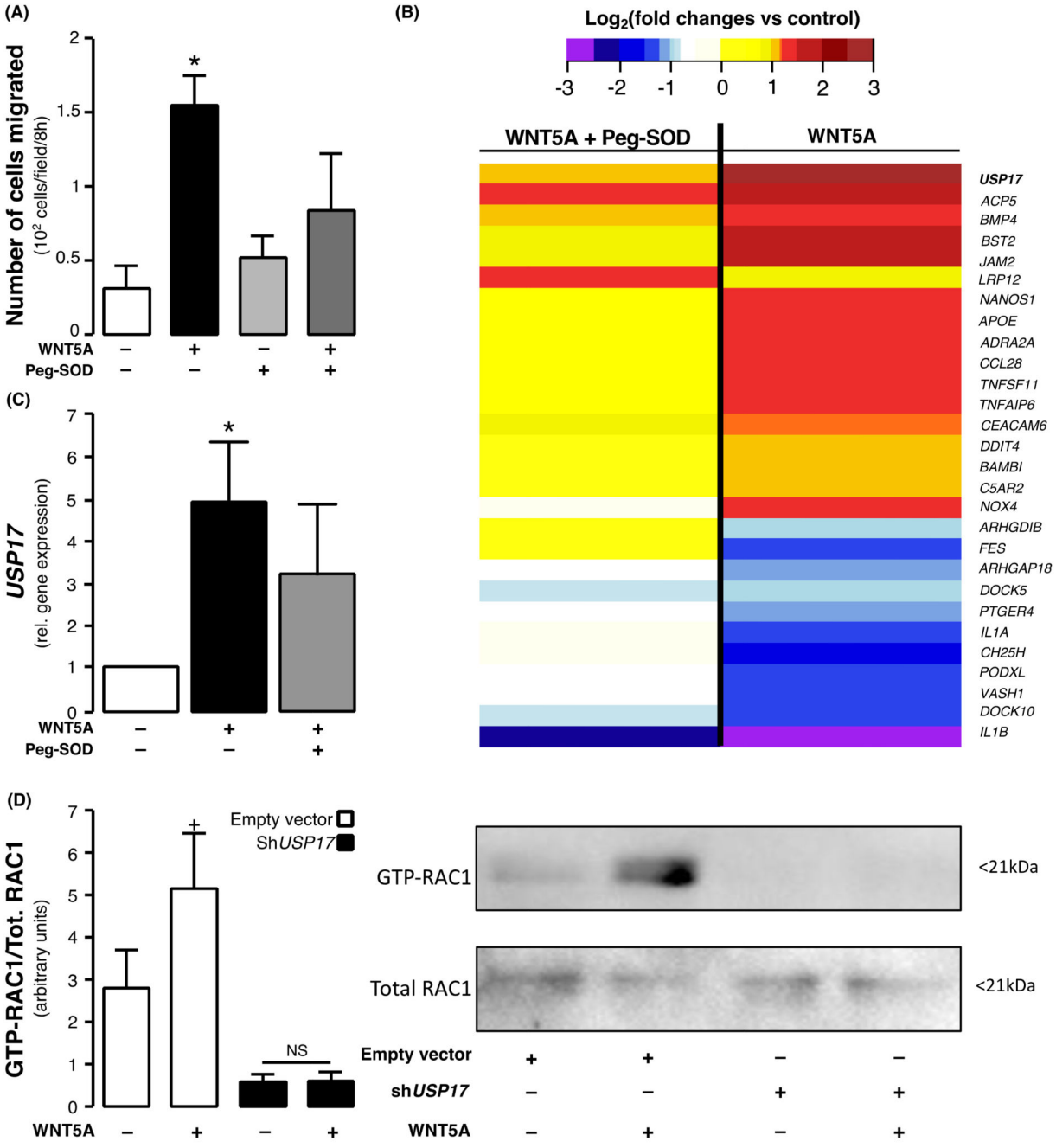

Fig. 8. USP17 as a link between WNT5A and vascular redox signaling.

(**A**) Migration of VSMCs incubated with peg-SOD, an intracellular scavenger of superoxide ($O_{2.}$-) production, (n = 5-8 pairs per intervention) and treated with WNT5A. (**B**) A subset of the WNT5A cell-motility differentially expressed genes of the microarray analysis were at least partially rescued by superoxide ($O_{2.}$-) anion scavenging with superoxide dismutase (peg-SOD) resulting in p-values>0.05 (n = 5 pairs, genes presented by descending mean fold change). (**C**) USP17 expression in VSMCs incubated with peg-SOD and treated with WNT5A (n = 10). (**D**) RAC1 activation in HeLa cells transfected with shUSP17 and treated

with WNT5A ($n = 8$). Data are presented as mean ± SEM in panels A, C and D. *$P < 0.05$ vs control by Wilcoxon signed rank test in panels A & C.+$P<0.05$ vs untreated empty vector control by Wilcoxon signed rank test; NS by Wilcoxon signed rank test for WNT5A -treated vs untreated sh*USP17* cells in panel D.

Europe PMC Funders Author Manuscripts